Precise Point Positioning requires consistent global products

H. P. Kierulf* Hans-Peter Plag†

Abstract

Precise Point Positioning (PPP) is increasingly used to compute time series of point motion in a global reference frame from continuously recording GPS receivers. Applications range from monitoring of infrastructure (including off-shore) over regional and global studies of surface displacements and strain to monitoring of sea level, ice load changes and other global change-related parameters. Most of the applications require a long-term stability (over order of 50 years) on the millimeter to sub-millimeter per year level. The results are thus particularly sensitive to temporal inhomogeneities of the reference frame or the global products (*satellite orbits and clocks*, SOC, as well as Earth rotation parameters). The IGS provides routinely highly accurate global products, which, combined with local GPS observations, give *ad hoc* access to the global reference frame nearly everywhere on the global.

In order to assess the long-term consistency of the IGS products with the ITRF2000, coordinate time series obtained with IGS precise SOC are compared to similar time series obtained with SOC provided by the *Jet Propulsion Laboratory*. The IGS products are found to introduce offsets in the coordinate time series at the transition from IGS97 to IGS00 (at 2001-12-02) equivalent to an offset of the frame origin of $+10$ mm in the z-coordinate. Secular trends determined from time series computed with the IGS and JPL products, respectively, differ in the order of $\pm 3 mm/yr$, which only partly can be attributed to a relative secular translation of the origins of the frames determined by the IGS and JPL global products. In the vertical component, JPL-based vertical trends on average appear to be larger by 1.3 mm/yr. This indicates and inconsistency of the PPP analysis and the computation of the IGS SOCs and also a potential effect of a trend in the relative scale of the IGS and JPL reference frames. The seasonal cycle in the vertical motion depends strongly on the global products used. This is due to different treatment of the geocenter variations in the frames determined by the IGS and JPL SOC.

1 Introduction

Monitoring of point motion is important for a wide range of applications. Displacements of the Earth's surface, for example, are cause by a number of geodynamic processes on local to global scale, and time series of point coordinates provide an important tool to study these process. Changes in sea level, ice sheets and other surface masses load and deform the solid Earth. Monitoring global change processes thus benefits from time series of displacements of the Earth's surface. For many studies, secular velocities are a main goal of the monitoring. Monitoring parameters relevant for global change studies, such as global sea level and changes in the water content of the troposphere, are the most demanding applications in terms of long-term stability. Large infrastructure such as off-shore platforms, bridges, and reservoir dams increasingly need to be monitored in order to assess their stability.

For most of these applications, access to a highly accurate, stable and consistent global reference frame is crucial. Most of the scientific applications require a stability on the 1 mm/yr level and studies of global sea level, for example, even need sub-millimeter per year in stability over long time intervals. The monitoring of off-shore infrastructure poses similar requirements (Plag, 2004).

The *International Earth Rotation and Reference Systems Service* (IERS) maintains the definition of the *International Terrestrial Reference System* (ITRS). Over the last decade, the ITRS has been realized through increasingly more accurate versions of the *International*

*Norwegian Mapping Authority, N-3507 Hønefoss, Norway, e-mail: halfdan.kierulf@statkart.no

†Norwegian Mapping Authority, now at Nevada Bureau of Mines and Geology & Seismological Laboratory, University of Nevada, Reno, USA, e-mail: hpplag@unr.edu

Terrestrial Reference Frame (ITRF). The subsequent versions of ITRF are based on combinations of solutions from the different space-geodetic techniques, thus making best use of the different characteristics of these techniques, as well as mitigating their deficiencies (see Altamimi et al., 2002, for more details). The most recent and presumably most accurate realization of the ITRS is ITRF2000 (Altamimi et al., 2002). ITRF2000 has been determined by the IERS through a weighted adjustment of solutions from the primary space geodetic techniques, such as *Very Long Baseline Interferometry* (VLBI), *Satellite Laser Ranging* (SLR), *Doppler Orbitography and Radiopositioning integrated by Satellites* (DORIS) and *Global Positioning System* (GPS). The result of the combination is a set of coordinates and velocities for the globally distributed network of ITRF points, which implicitly determine the orientation, scale and origin of the coordinate system as well as their rates.

Access to the ITRF can be obtained through measurements relative to points with known ITRF coordinates. Alternatively, satellite geodetic techniques like GPS and in the future Galileo allow access to ITRF *ad hoc* with high accuracy through global products (i.e. the satellite orbits and clocks, SOC, and Earth Rotation Parameters, ERP) given relative to a global network of reference stations tracking the satellites. However, depending on the tracking stations and the methodology used to achieve the connection of the global products to ITRF, the different global products vary in accuracy and their long-term stability relative to ITRF.

The *International GNSS Service* (IGS) maintains a global tracking network for the GPS, which includes today more than 300 stations. This network has the densest coverage of all ground networks of the space-geodetic techniques contributing to the ITRF. Consequently, GPS contributes significantly to the determination and subsequent monitoring of each ITRF version.

Based on the observations from the tracking network, the IGS provides SOC and ERP as well as the time series of the reference coordinates for the IGS tracking stations (Ray et al., 2004). The SOC and ERP that can be used to monitor coordinates of a point either through Precise single Point Positioning (PPP, Zumberge et al., 1997) relative to the SOC or by using additional information from nearby reference sites. GPS in combination with the IGS products thus allows the determination of point coordinates relative to the ITRF on any location of the Earth surface with nearly the same accuracy. Currently GPS is the only technique that provides this global, high-accuracy access to ITRF.

Increasingly, PPP is used to get coordinates of new points or to determine time series of point coordinates from continuously operated GPS (CGPS) receivers. Compared to the other standard approach in space-geodetic analysis, i.e. a processing of a network of stations, PPP has the advantage that it does not depend explicitly on local or regional reference points and that it requires comparably little resources. Moreover, the resulting time series are expressed in the reference frame defined by the global products and not dependent on any local or regional points. PPP is, however, more affected by deficiencies of the station motion model assumed in the analysis, as well as error in the SOC. Furthermore, inconsistencies between the PPP analysis and the one performed to determine the SOC can easily introduces a bias in the results of the PPP.

In most PPP application, the SOC provided by the *Jet Propulsion Laboratory* (JPL) are used, thus ensuring homogeneity of the global products and the PPP analysis. However, Ray et al. (2004) recommended a study to assess the performance of the IGS products in PPP. Here we concentrate on a particular aspect, i.e. the effect of the transition from ITRF97 (Boucher et al., 1999) to ITRF2000 and the potential bias due to this transition.

The resulting accuracy of the coordinate time series depends of course on the accuracy of the IGS products with respect to ITRF and on the accuracy of the ITRF itself. As pointed out above, for most applications the long-term stability is a key requirement. To give an example it is noted that an unaccounted secular translation of the origin of the reference frame with respect to the center of mass of the Earth system of as little as 1 mm/yr could introduce an error in global sea level of 0.4 mm/yr (Plag & Kierulf, 2005). Consequently, detailed knowledge of the long-term stability of the IGS products with respect to the ITRF is of crucial interest. Moreover, deficiency of the ITRF with respect to some of the conventions underlying the ITRS (McCarthy & Petit, 2003) would also compromise the accuracy of the coordinate time series as well as the secular velocity field. In particular, discrepancies between the origin of the reference frame (either ITRF itself or the frame determined through the SOCs) and the physical geocenter as well as deviations from the so-called No-Net-Rotation condition for the Earth's surface would hamper the geophysical interpretation of the coordinate time series and the

velocity field determined from them.

In the following, we first give details of the relation between ITRF2000 and the reference frames determined by the IGS products with focus on the motion of the origin of these frames with respect to each other. We then consider the potential biases introduced by these products into coordinate time series determined from Continuous GPS (CGPS) observations using the PPP approach. We assess the biases due to IGS products through comparison to homogeneous SOCs provided by JPL.

2 IGS global products and their associated reference frames

A recent overview over the IGS products and the reference frames associated with them is given by Ray et al. (2004). The IGS determines precise weekly GPS coordinates for the tracking stations of the global IGS network in a reference frame closely aligned to ITRF2000, which is denoted as IGb00 (IGS00, before January, 11, 2004). IGb00 is a combined reference frame based on a least squares fit of the individual reference frames determined by the IGS *Analysis Centers* (AC). The individual free network solutions are related to IGb00 through rigid Helmert transformation

$$\vec{X}' = \vec{X} + \vec{T} + R \cdot \vec{X} \tag{1}$$

where the Cartesian vectors $\vec{X}'$ and $\vec{X}$ are the position in the free solutions and IGb00, respectively, and $\vec{T}$ describes a translation of the origin of the individual solution with respect to the origin of IGb00. The matrix R is given by

$$R = \begin{pmatrix} S-1 & -R_Z & R_Y \\ R_Z & S-1 & -R_X \\ -R_Y & R_X & S-1 \end{pmatrix} \tag{2}$$

where the components R_i describe the rotation and S is the scale of the free solution with respect to IGb00. IGS uses about 100 reference frame stations for the determination of the transformation parameters in eq. (1), while ensuring that IGb00 keeps the internal consistency of the combined GPS solution. Consequently, these IGb00 reference coordinates are internally more consistent than the original ITRF2000 coordinates, while in orientation, translation and scale (including rates), IGb00 and ITRF2000 are equivalent. Since IGb00 is based on a subset of the global ITRF network and on only one technology, IGb00 can be considered as a single-technique approximation to ITRF2000.

Currently, the products most often used to access ITRF2000 or, synonymously, IGb00 are the precise SOC and ERP provided by the IGS. These products are given in a specific *IGS precise SOC frame* denoted here as IGS-P00. This frame is not equivalent to IGb00 (note that the IGS rapid products are, in fact, given in IGb00). Since autumn 1998, the individual solutions provided by the IGS ACs are either unconstrained (i.e. for none of the tracking stations the coordinates are fixed within a certain limit to the nominal ITRF2000 values) or the constraints are removed at the combination level. Since February 27, 2000, the rigorous IGS SINEX station/ERP combinations have started. Subsequent to that date, all IGS combined final products (SOC and ERP) are fully consistent and minimally constrained with respect to the IGb00 reference frame. The precise SOC and ERP frame, i.e. IGS-P00, is minimally constrained to ITRF using the relation

$$\vec{X}' = \vec{X} + \tilde{R} \cdot \vec{X} \tag{3}$$

where

$$\tilde{R} = \begin{pmatrix} 0 & -R_Z & R_Y \\ R_Z & 0 & -R_X \\ -R_Y & R_X & 0 \end{pmatrix} \tag{4}$$

is a rotation matrix. Thus, IGS-P00 is constrained to IGb00 only in orientation but not in translation and scale. Consequently, the translation and scale variation between IGS-P00 and IGb00 (or ITRF2000) can be interpreted as a deviation of the most accurate GPS-based realization of ITRS with respect to the multi-technique ITRF2000.

Since IGS-P00 is only constrained to ITRF using eq. (3), IGS-P00 approximates neither ITRF2000 nor IGb00, but is a reference frame with scale determined by the GPS system itself and the origin in the Earth center of mass as sensed by the GPS system alone (Ray et al., 2004). Thus the main difference between IGS-P00 and ITRF2000 is a movement of the (observed by GPS only) IGS-P00 geocenter (identical to the IGS-P00 origin) with respect to ITRF2000 resulting in all velocities given in IGS-P00 being different from those in ITRF2000.

Some of the IGS ACs provide own sets of global products. One example is NASA's JPL, which pro-

vides highly accurate and consistent SOC. In contrast to the IGS precise products, JPL precise SOC and ERP are given in a loosely constrained reference frame. Consequently, coordinates determined by JPL precise products have to be transformed to ITRF2000 using a Helmert transformation (see eq. 1). JPL provides daily estimates of the seven-parameter transformations from the free network solution to ITRF2000. These parameters are determined on the basis of a global network of some 50 stations, for which the ITRF2000 coordinates are used. Thus, the JPL precise products together with these transformation parameters determine a reference frame (denoted here as JPL-P00), which is well aligned to ITRF2000 with the translation of the origins being numerically equal to zero. Consequently, station velocities for ITRF sites determined with the JPL precise products agree well with their ITRF2000 velocities.

3 Methodology

In order to assess the effect of the different global products on velocities determined from CGPS time series, we have processed a globally distributed subset of IGS stations using both IGS-P00 and JPL-P00 global products. The time window is 2000.0 to 2004.0, i.e. four years. This allows to determine secular trends not significantly biased by any seasonal signal (Blewitt & Lavallée, 2002).

The time series of coordinates are computed with GIPSY-OASIS using the PPP approach, a sampling interval of 300 s (for IGS products before 2000-11-05 of 900 s), and elevation mask of 10 degrees. The station motion model agrees with the IERS conventions (McCarthy & Petit, 2003). Ocean tidal loading is included in the station motion model as derived from Scherneck & Bos (2001) using the ocean tidal model GOT00.2.

For the PPP with IGS products, we follow the recommendations in Kouba (2003). IGS made a transition from IGS97 to IGS00 at 2001-12-02, and prior to that date all parameters are referred to IGS97. Before 2001-12-02, IGS precise SOC and ERPs are minimally constrained to IGS97. All transformation parameters exhibit an offset at that date. The offset of the origin, which is particularly large in the Z-component, is accounted for in the *a priori* transformation provide by IGS for the transformation of the SOC prior to the transition date from ITRF97 to ITRF2000 (see Table 3). For the transformation from ITRF97 to IGS00/IGb00, IGS provides the program trnfsp3n, which utilizes the transformation given by Weber (2001). Any error in this transformation will show up in coordinate time series e.g. as an offsets and, possibly, a change in trend at the transition date.

For the PPP with JPL products, we have used the Helmert transformations provided by JPL to transform the free network solutions to the JPL-P00 approximation of ITRF2000. In addition to this standard method, we also computed time series where only the three rotation parameters of the transformation are used (equivalent to eq. 3). This latter approach results in a reference frame based on JPL precise SOCs, which is as closely as possible aligned to IGS-P00.

For the determination of highly accurate trends, the function

$$f(t) = a + bt + \alpha H(t - t_{\mathrm{T}}) + \sum_{i=1}^{2} A_i \sin(\omega_i t) + B_i \cos(\omega_i t), \quad (5)$$

is fitted to the coordinate time series in a weighted least squares fit, with t being time, H a Heaviside function, t_{T} the time of the transition from ITRF97 to ITRF2000, and ω_1 and ω_2 the angular frequencies of an annual (denote here as Sa) and semi-annual (Ssa) harmonic constituent, respectively. More over, additional offsets are included in the model function wherever known discontinuities exist.

4 Inhomogeneity due to transition from ITRF97 to ITRF2000

Initially, we focus on height time series, since for many monitoring applications (including sea level), the height component is the most important one. Figure 1 shows four examples of the height time series obtained with the different SOC. The stations shown are Ny-Ålesund, Svalbard, Davis, Antarctica, Irkutsk, Russia, and Yellowknife, Canada.

All coordinate time series computed with the IGS precise SOC exhibit a jump at the date of the transition from IGS97 to IGS00 (Table 1), which may vary from -13 mm to $+13$ mm. The JPL products do not have a temporal inhomogeneity associated with the transition from ITRF97 to ITRF2000 since the transformation

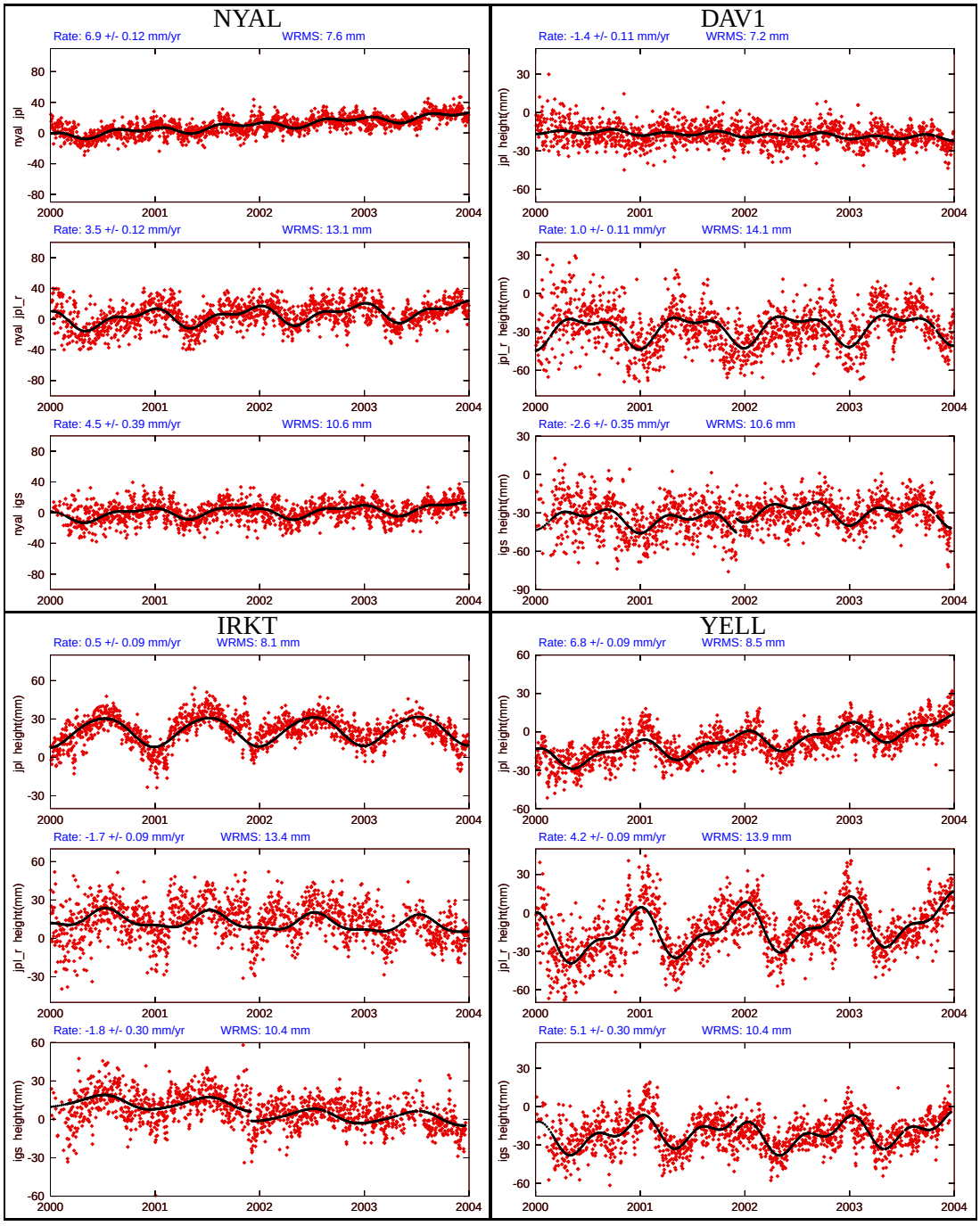

Figure 1: IGS- and JPL-based time series for height.

Left top: Ny Ålesund, Svalbard; right top: Davis, Antarctica; lower left: Irkutsk, Russia; lower right: Yellowknife, Canada. For each station, top: JPL global products using full 7-parameter-transformation (JPL-P00 products), middle: JPL global products using only the three rotation parameters of the transformation to ITRF2000, bottom: IGS precise products (IGS-P00 products).

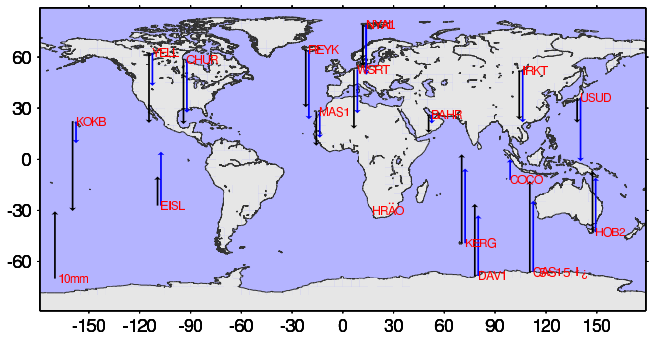

Figure 2: Offsets in height time series at the IGS transition from IGS97 to IGS00.
The arrows are the offset in height at 2001-12-02. Black arrows are offsets in height using IGS SOCs. Blue errors are the same offsets corrected for the offsets found in height time series using JPL SOCs.

parameters from the free network to ITRF2000 were re-determined for the time before the transition date. Therefore, we also determined the offsets in the IGS-P00 time series relative to the offsets found at the same date in the JPL-P00 time series. The (artificial) jumps in the JPL-based time series reach up to ± 4 mm, thus indicating the uncertainty in the jumps determined by using the model function (5). In Figure 2, the geographical pattern of the offsets in the IGS-based height time series is shown. This pattern is roughly consistent with a translation of the origin mainly along the z-axis. Plotting the offsets as function of latitude demonstrates that the offsets are consistent with a translation of the origin along the z-axis of approximately 12 mm (Figure 3).

In order to determine the translation of the origin at the time of the transition more accurately, we determine the offsets in time series of deviations in the geocentric coordinates x, y, z (Table 2). The relative offsets (i.e. relative to the offsets found for the JPL-based time series) do not different significantly from those determined for the IGS-based time series and the means and median are largely unaffected.

For the x- and y-component, the residual offsets are not significantly different from zero. However, in the z-component, we find a residual mean offset of 9.6 ± 2.8 mm. This offset of the IGS-P00 origin with respect to the IGS97 origin transformed to IGS00 explains most of the offsets in the coordinate time series. The offset has to be attributed to an inaccuracy of the transformation provided by Weber (2001). However, this transformation is not necessarily appropriate for the transformation of the IGS precise orbits given prior to the transition date with respect to IGS97 into the frame of the IGS precise SOC after the transition date, which are given in IGS-P00 and not IGS00. Consequently, using IGS SOC as sole tool to access ITRF2000 (i.e. without the use of additional ITRF2000 reference coordinates of IGS stations) results in a significant error of secular velocities if the time window includes the transition date. This error can be mitigated by determining a more appropriate transformation between IGS-P00 and IGS97 on the basis of a sufficient number of reference stations.

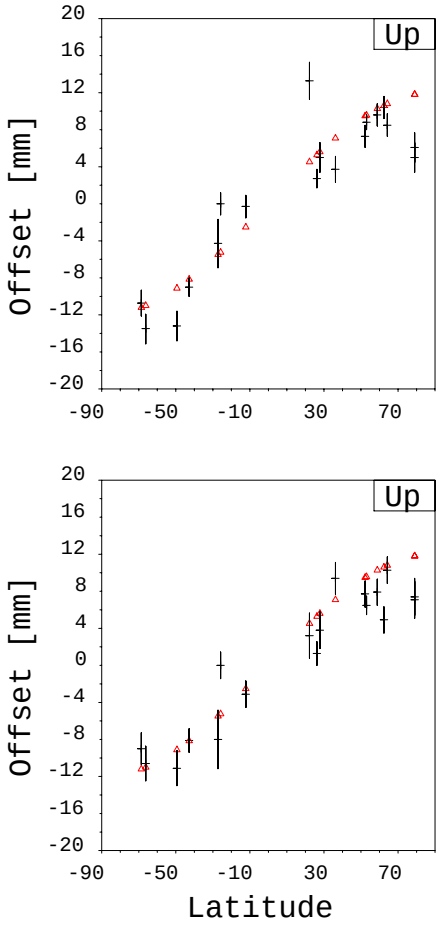

Figure 3: Latitude-dependency of the offsets in height time series at the IGS transition from IGS97 to IGS00.
Upper diagram: Offsets in IGS-based time series. Lower diagram: Offsets corrected for similar offsets in JPL-based time series. The triangles are the offsets due to a translation of the origin along the z-axis of 12 mm.

Table 1: Offsets in height time series at the transition from IGS97 to IGS00.

Station	Longitude	Latitude	IGS	JPL	IGS - JPL
	degrees	degrees	mm	mm	mm
BAHR	50.61	26.21	2.7 ± 1.0	1.4 ± 0.8	1.3 ± 1.3
CAS1	110.52	-66.28	-13.5 ± 1.6	-2.9 ± 1.0	-10.6 ± 1.9
CHUR	-94.09	58.76	9.6 ± 1.2	1.7 ± 0.8	7.9 ± 1.4
COCO	96.83	-12.19	-0.3 ± 1.2	2.9 ± 0.8	-3.1 ± 1.4
DAV1	77.97	-68.58	-10.7 ± 1.4	-1.8 ± 1.0	-9.0 ± 1.7
EISL	-109.38	-27.15	-4.3 ± 2.6	3.7 ± 1.8	-8.0 ± 3.2
HOB2	147.44	-42.80	-9.0 ± 1.0	-0.9 ± 0.8	-8.1 ± 1.3
HRAO	27.69	-25.89	0.0 ± 1.2	0.0 ± 0.8	0.0 ± 1.4
IRKT	104.32	52.22	7.3 ± 1.2	-0.3 ± 0.8	7.7 ± 1.4
KERG	70.26	-49.35	-13.2 ± 1.6	-2.1 ± 1.0	-11.1 ± 1.9
KOKB	-159.66	22.12	13.3 ± 2.0	10.1 ± 1.4	3.2 ± 2.4
MAS1	-15.63	27.76	5.0 ± 1.6	1.2 ± 1.2	3.8 ± 2.0
NYA1	11.87	78.93	6.1 ± 1.6	-1.3 ± 1.2	7.4 ± 2.0
NYAL	11.87	78.93	5.0 ± 1.6	-2.2 ± 1.2	7.1 ± 2.0
REYK	-21.96	64.14	8.5 ± 1.2	-1.8 ± 0.8	10.3 ± 1.4
USUD	138.36	36.13	3.7 ± 1.4	-5.7 ± 1.0	9.4 ± 1.7
WSRT	6.60	52.91	8.8 ± 0.8	2.3 ± 0.6	6.5 ± 1.0
YELL	-114.48	62.48	10.4 ± 1.2	5.5 ± 0.8	4.9 ± 1.4

5 Effect of global products on secular trends

The trends determined for the IGS-P00 and JPL-P00 height time series are for most sites significantly different (Table 4), with the differences being of the order of ± 3 mm/yr. However, considering the mean of the trend differences for the geocentric components does not result in a significant translation of the origin of JPL-P00 with respect to IGS-P00 (Table 5). Thus, the spatial pattern of the trend differences is not consistent with a secular translation of the origins of JPL-P00 and IGS-P00 with respect to each other. Such a translation is, however, expected on the basis of the translation parameters between the free JPL solutions and JPL-P00 and between IGS-P00 and IGb00 (Plag & Kierulf, 2005). Therefore, we conclude that other factors introduce noise in the trends of the IGS and JPL-based time series that mask the origin translations.

For the height component, the JPL-based trends are on average about 1.3 mm/yr larger than those based on IGS SOC. We suspect that inconsistencies between the computation of the IGS-P00 SOC and the PPP lead to additional effects biasing particularly the vertical component. Thus, differences in the cut-off elevation angle could introduce a bias in the trend (Kierulf et al., 2001). Moreover, a secular variation in the relative scale between the two frames could also contribute to this bias.

6 Effect of global products on the seasonal signal

Recently, the seasonal signal in CGPS time series has been described, for example, by Blewitt et al. (2001) and Dong et al. (2002). This signal potentially depends strongly on the reference frame chosen. For example, in analysis using regional reference frames or regional filtering (see e.g. Wdowinski et al., 1997; Nikolaides, 2002; Wdowinski et al., 2004), the seasonal cycle is largely reduced due to its long-wave length components. In PPP analysis, the global products and the reference frame defined by them are crucial for the seasonal signal in the time series, as is demonstrated in Figure 1: For each station, the seasonal signals are rather different both in amplitude and shape for the three dif-

Table 2: Offsets in time series of geocentric coordinates at the transition from IGS97 to IGS00.

Station	X		Y		Z	
	IGS	IGS-JPL	IGS	IGS-JPL	IGS	IGS-JPL
	mm	mm	mm	mm	mm	mm
CAS1	2.31± 0.39	3.48± 0.47	-2.33± 0.39	-3.00± 0.47	15.16± 0.65	13.75± 0.78
CHUR	3.66± 0.30	2.49± 0.37	1.62± 0.33	2.18± 0.40	10.10± 0.45	7.19± 0.55
COCO	0.57± 0.29	-1.46± 0.35	0.51± 0.50	-3.23± 0.61	7.94± 0.15	7.56± 0.19
DAV1	3.34± 0.32	2.37± 0.39	-1.19± 0.34	-2.87± 0.42	11.72± 0.58	11.60± 0.71
EIS1	-0.24± 0.61	3.14± 0.74	5.16± 0.96	0.83± 1.18	11.06± 0.56	11.31± 0.69
HOB2	1.09± 0.33	0.27± 0.40	-2.97± 0.29	-3.12± 0.35	10.23± 0.31	10.77± 0.38
IRKT	1.10± 0.32	1.84± 0.39	1.65± 0.40	2.47± 0.49	5.25± 0.46	7.26± 0.55
KERG	1.24± 0.43	3.30± 0.52	-5.27± 0.55	-7.44± 0.67	14.31± 0.59	13.20± 0.71
KOKB	-8.17± 0.79	0.93± 0.97	-2.55± 0.53	-4.70± 0.65	11.44± 0.37	11.09± 0.45
MAS1	0.31± 0.70	-1.66± 0.86	-1.51± 0.41	-3.27± 0.50	9.36± 0.38	8.09± 0.47
NYA1	3.85± 0.28	4.27± 0.34	3.24± 0.28	1.45± 0.34	6.25± 0.72	5.06± 0.88
NYAL	0.47± 0.29	4.01± 0.35	2.73± 0.28	1.75± 0.34	6.24± 0.73	5.17± 0.90
REYK	0.79± 0.30	3.94± 0.37	0.40± 0.28	0.72± 0.34	9.01± 0.53	8.24± 0.65
USUD	3.04± 0.43	0.53± 0.52	1.21± 0.38	3.97± 0.47	5.93± 0.34	9.80± 0.41
WSRT	3.53± 0.28	1.83± 0.34	0.49± 0.22	-0.84± 0.26	8.83± 0.33	6.32± 0.40
YELL	0.46± 0.31	2.42± 0.37	-1.73± 0.32	3.55± 0.39	10.74± 0.50	6.69± 0.60
Mean	1.08± 2.74	1.98± 1.77	-0.03± 2.59	-0.72± 3.20	9.60± 2.78	8.94± 2.66
Median	0.6< 1.1< 2.3	1.8< 2.4< 3.1	-1.5< 0.4< 1.2	-3.0< -0.1< 1.5	8.8< 9.7< 10.7	7.3< 8.2< 10.8

Table 3: Origin translation at the transition from IGS97 to IGS00.
In the first column the a priori *offsets at the transition from ITRF97 to ITRF2000 from Weber (2001) are given. The second column gives the same values determined from the time series of the geocenter motion (Plag & Kierulf, 2005). The third and fourth column are the mean and median, respectively, of the offsets determined for the IGS-based time series of station coordinates (see Table 2). The last column gives the mean offsets for the differences between IGS-P00 and JPL-P00 offsets. All values are in millimeters. The confidence interval for the median is for 95 %.*

	Offset origin		Residual offset		Diff. Offsets
	IGS	Plag & Kierulf (2005)	Mean	Median	Mean
X	-4.5 ± 4.1	-7.1 ± 1.2	1.0 ± 2.7	$0.6 < 1.1 < 2.3$	1.9 ± 1.8
Y	-2.4 ± 5.0	-6.0 ± 1.2	0.0 ± 2.5	$-1.5 < 0.4 < 1.2$	-0.7 ± 3.2
Z	26.0 ± 7.5	21.3 ± 3.2	9.6 ± 2.8	$8.8 < 9.7 < 10.7$	8.9 ± 2.7

ferent time series of height changes. In Table 6, we compare the annual (Sa) and semi-annual (Ssa) constituents determined in the fit of eq. (5) to the IGS- and JPL-based height time series, respectively. To illustrate the considerable differences in amplitudes and phases of the Sa and Ssa, in Figure 4 we have plotted the ratios of these parameters for the IGS- and JPL-based solutions. Only for the phase of Sa an agreement is found almost everywhere. For most stations, the Sa amplitude is lower in the JPL series than in the IGS series. For Ssa, for most stations, the JPL amplitude is only about half the IGS amplitude. Partly, these differences can be attributed to the differences in the seasonal variations of the origins of the two frames. While JPL-P00 is fully

Table 4: Secular trends for height time series determined for the CGPS stations.
Columns denoted by JPL and IGS give the linear trends estimated from time series computed with JPL and IGS SOC, respectively. Diff. is the difference of the trends given as JPL - IGS. Mean and Median are for all samples, while Mean and Medium* are for the samples excluding KOKB.*

Station	JPL mm/yr	IGS mm/yr	Diff. mm/yr
BAHR	-1.0 ± 0.2	-2.6 ± 0.5	1.6 ± 0.5
CAS1	-0.5 ± 0.2	-1.8 ± 0.7	1.3 ± 0.7
CHUR	11.5 ± 0.2	11.3 ± 0.6	0.2 ± 0.6
COCO	3.3 ± 0.2	3.5 ± 0.5	-0.2 ± 0.5
DAV1	-1.4 ± 0.2	-2.6 ± 0.7	1.2 ± 0.7
EISL	1.7 ± 0.4	2.9 ± 1.3	-1.2 ± 1.4
HOB2	2.8 ± 0.1	1.2 ± 0.5	1.6 ± 0.5
HRAO	1.0 ± 0.2	-1.6 ± 0.6	2.6 ± 0.6
IRKT	0.5 ± 0.2	-1.8 ± 0.6	2.3 ± 0.6
KERG	-0.7 ± 0.3	-2.0 ± 1.1	1.3 ± 1.1
KOKB	1.7 ± 0.2	5.7 ± 0.8	-4.0 ± 0.8
MAS1	3.4 ± 0.3	4.7 ± 0.9	-1.3 ± 0.9
NYA1	6.5 ± 0.2	4.5 ± 0.8	2.0 ± 0.8
NYAL	6.9 ± 0.2	4.5 ± 0.8	2.4 ± 0.8
REYK	-1.1 ± 0.2	-1.6 ± 0.8	0.5 ± 0.8
USUD	-3.1 ± 0.2	-1.8 ± 0.7	-1.3 ± 0.7
WSRT	-1.6 ± 0.1	-2.5 ± 0.4	0.9 ± 0.4
YELL	6.8 ± 0.2	5.1 ± 0.6	1.7 ± 0.6
Mean	2.0 ± 3.7	1.4 ± 3.9	0.6 ± 1.7
Median	$-0.7 < 1.4 < 3.3$	$-1.8 < -0.2 < 4.5$	$0.2 < 1.3 < 1.6$
Mean*	2.1 ± 3.8	1.1 ± 3.9	0.9 ± 1.2
Median*	$-0.7 < 1.0 < 3.3$	$-1.8 < -1.6 < 3.5$	$0.5 < 1.3 < 1.6$

aligned to ITRF2000 through a network of about 50 stations, the origin of IGS-P00 is free to follow the geocenter as sensed by GPS alone. This results in a seasonal translation of the two origins with respect to each other. However, this translation does not explain all the differences shown in Table 6 and Figure 4. Therefore, inconsistencies in the PPP analysis and the computation of the products appears to add spatially variable seasonal signals to the time series, that are difficult to interpret geophysically.

7 Conclusions

IGS precise products have a temporal inhomogeneity of the order of 10 mm associated with the transition from IGS97 to IGS00 and thus can not be used directly to determine highly accurate trends for time series including the transition date. This offset is mainly due to an inconsistency of the necessary transformation of the IGS SOC prior to the transition date from IGS97 to IGS00. After the transition, the IGS precise orbits are given in IGS-P00, which is not identical to IGS00. Therefore, the transformation from IGS97 to IGS00 provided by IGS (Weber, 2001) is not appropriate for the transformation of the precise SOC. If IGS SOC are to be used for PPP, then for times prior to the transition to ITRF2000, the determination of a new transformation for the SOC from IGS97 to IGS-P00 is needed. For that, a procedure similar to the transformation of JPL's free network solutions to ITRF2000 can be applied.

Station velocities determined on the basis of IGS precise products for ITRF reference sites (corrected for

Table 5: Difference in trends in time series of geocentric coordinates determined with IGS and JPL SOC.

Station	X		Y		Z	
	IGS	IGS-JPL	IGS	IGS-JPL	IGS	IGS-JPL
	mm/yr	mm/yr	mm/yr	mm/yr	mm/yr	mm/yr
CAS1	1.60± 0.17	0.52± 0.20	-9.71± 0.18	-0.18± 0.21	-1.69± 0.29	1.96± 0.34
CHUR	-17.47± 0.14	1.49± 0.17	-6.76± 0.16	1.92± 0.19	6.81± 0.21	-2.64± 0.25
COCO	-46.23± 0.14	0.33± 0.17	9.58± 0.23	0.72± 0.27	45.60± 0.07	-1.10± 0.09
DAV1	1.96± 0.15	0.64± 0.17	-6.57± 0.16	-0.21± 0.19	0.42± 0.27	2.07± 0.32
EIS1	66.15± 0.29	-0.80± 0.34	-21.54± 0.49	-1.81± 0.57	-6.00± 0.28	-0.77± 0.33
HOB2	-39.89± 0.15	0.09± 0.17	9.21± 0.13	-0.31± 0.15	39.53± 0.14	1.44± 0.17
IRKT	-22.79± 0.15	2.41± 0.17	0.38± 0.18	-0.16± 0.22	-8.95± 0.21	-2.96± 0.25
KERG	-7.12± 0.29	0.39± 0.33	-0.48± 0.37	-0.47± 0.43	0.32± 0.39	1.59± 0.45
KOKB	-12.48± 0.41	0.29± 0.48	61.98± 0.27	-2.53± 0.31	32.82± 0.18	1.87± 0.21
MAS1	0.30± 0.39	0.24± 0.46	15.49± 0.22	-0.81± 0.26	17.32± 0.21	0.86± 0.25
NYA1	-12.96± 0.13	1.41± 0.15	8.45± 0.12	0.91± 0.14	7.31± 0.32	-2.74± 0.38
NYAL	-11.99± 0.13	1.47± 0.15	7.94± 0.12	0.88± 0.14	7.53± 0.33	-2.52± 0.39
REYK	-21.85± 0.19	1.98± 0.22	-3.29± 0.17	2.08± 0.20	7.32± 0.32	-1.02± 0.38
USUD	-2.11± 0.22	-1.63± 0.27	3.29± 0.19	1.01± 0.23	-10.36± 0.17	1.38± 0.20
WSRT	-14.30± 0.13	0.07± 0.15	16.31± 0.10	0.11± 0.12	6.57± 0.15	-2.64± 0.18
YELL	-20.04± 0.14	1.87± 0.16	-3.86± 0.14	3.00± 0.17	-0.59± 0.22	-3.24± 0.26
Mean		0.67± 1.02		0.26± 1.37		-0.53± 2.00
Median		0.3< 0.5< 1.4		-0.2< 0.0< 0.9		-2.5< -0.9< 1.4

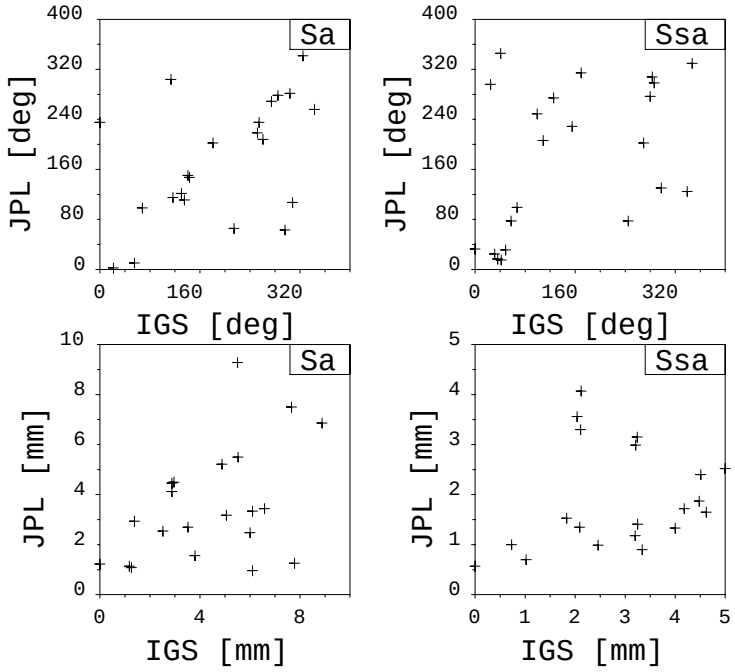

Figure 4: Comparison of seasonal constituents in IGS- and JPL-based height time series.
Left diagrams: annual constituents (Sa), right diagram: semi-annual constituents (Ssa). Upper row: comparison of phases, lower row comparison of amplitudes.

Table 6: Comparison of seasonal constituents in IGS- and JPL-based height time series.
The amplitudes and phases of the annual and semi-annual constituents are determine in the fit of eq. (5) to the height time series. Amplitudes are in mm, phases in degrees.

Station	Annual Constituent				Semi-Annual Constituent			
	IGS		JPL		IGS		JPL	
	Ampl.	Phase	Ampl.	Phase	Ampl.	Phase		
BAHR	7.5 ± 0.2	281.3 ± 1.4	1.4 ± 0.2	206.4 ± 7.8	7.7 ± 0.3	303.8 ± 2.1	2.1 ± 0.3	109.0 ± 7.4
CAS1	2.5 ± 0.2	235.2 ± 5.7	1.2 ± 0.2	298.3 ± 12.1	6.0 ± 0.4	254.1 ± 3.7	3.2 ± 0.4	286.5 ± 6.7
CHUR	5.5 ± 0.2	202.7 ± 2.1	1.7 ± 0.2	77.3 ± 6.6	5.5 ± 0.3	180.7 ± 3.0	4.2 ± 0.3	57.4 ± 3.9
COCO	2.7 ± 0.2	341.4 ± 3.8	1.3 ± 0.2	228.7 ± 7.3	3.5 ± 0.3	324.6 ± 4.5	4.0 ± 0.3	155.3 ± 3.9
DAV1	1.0 ± 0.2	207.9 ± 14.5	1.7 ± 0.2	277.0 ± 8.4	6.1 ± 0.4	260.8 ± 3.5	4.6 ± 0.4	280.0 ± 4.4
EISL	4.1 ± 0.4	2.1 ± 5.9	2.5 ± 0.4	274.1 ± 9.5	2.9 ± 0.6	21.7 ± 12.8	5.0 ± 0.6	125.3 ± 7.1
HOB2	1.6 ± 0.2	62.9 ± 6.0	1.0 ± 0.2	130.5 ± 9.9	3.8 ± 0.3	296.0 ± 3.9	2.5 ± 0.2	297.9 ± 5.8
HRAO	4.5 ± 0.2	111.2 ± 2.6	0.9 ± 0.2	99.6 ± 13.1	2.9 ± 0.3	135.4 ± 6.2	3.3 ± 0.3	67.4 ± 5.2
IRKT	11.1 ± 0.2	269.2 ± 1.1	1.0 ± 0.2	296.1 ± 11.4	5.0 ± 0.3	274.5 ± 3.6	0.7 ± 0.3	25.2 ± 24.7
KERG	1.3 ± 0.2	218.5 ± 10.4	1.9 ± 0.2	307.8 ± 6.9	7.8 ± 0.4	252.0 ± 2.7	4.5 ± 0.3	283.0 ± 4.3
KOKB	5.2 ± 0.3	10.5 ± 2.8	2.4 ± 0.3	24.6 ± 6.1	4.9 ± 0.4	55.2 ± 5.0	4.5 ± 0.4	30.8 ± 5.2
MAS1	1.1 ± 0.3	65.3 ± 14.8	2.3 ± 0.3	124.9 ± 6.6	1.3 ± 0.4	214.1 ± 19.6	6.1 ± 0.4	339.3 ± 3.6
NYA1	3.3 ± 0.3	150.2 ± 4.5	3.0 ± 0.3	17.1 ± 4.9	6.1 ± 0.4	140.6 ± 3.7	3.2 ± 0.4	36.0 ± 6.7
NYAL	3.4 ± 0.3	146.9 ± 4.5	3.1 ± 0.3	14.9 ± 4.9	6.6 ± 0.4	143.2 ± 3.6	3.2 ± 0.4	42.0 ± 6.9
REYK	3.2 ± 0.2	121.3 ± 3.7	1.4 ± 0.2	329.8 ± 8.1	5.1 ± 0.3	130.1 ± 3.4	3.3 ± 0.3	347.2 ± 5.1
USUD	4.5 ± 0.2	278.1 ± 2.9	3.3 ± 0.2	345.4 ± 3.9	2.9 ± 0.3	285.0 ± 6.8	2.1 ± 0.3	40.6 ± 8.9
WSRT	1.1 ± 0.2	98.1 ± 7.9	0.7 ± 0.2	202.6 ± 12.8	1.2 ± 0.2	67.8 ± 11.3	1.0 ± 0.2	269.4 ± 12.4
YELL	6.9 ± 0.2	115.4 ± 1.7	3.7 ± 0.2	31.0 ± 3.0	8.9 ± 0.3	116.7 ± 2.0	7.1 ± 0.3	48.4 ± 2.4

the effect of the transition jump) do not agree well with their ITRF2000 velocities, with the differences being as large as ± 3 mm/yr. Vertical secular trends for the JPL based height time series are on average 1.3 mm/yr larger than those for the IGS-based time series. For the JPL SOC, consistency between these SOC and the subsequent PPP is ensured. This is not the case for the IGS SOC, which are a combined product. Most likely, inconsistencies between the IGS SOC and the PPP lead to the differences in the secular trends.

The different alignment of the two frames IGS-P00 and JPL-P00 to ITRF2000 leads to rather different seasonal signals in PPP time series based on these two SOC. Therefore, any geophysical interpretation of the seasonal signals needs to carefully consider the potential effect of the reference frame on the seasonal signals.

Acknowledgments

The authors would like to thank Jim Ray and Geoff Blewitt for helpful discussions. The authors also thank the JPL for making the GPS-related products freely available. The present study, though critical of the IGS products, would not have been possible without the IGS as would not have been many of the astonishing scientific results achieved over the last decade in space geodesy. Therefore, the authors would like to acknowledge the important service that the IGS community has provided to Earth sciences.

References

Altamimi, Z., Sillard, P., & Boucher, C., 2002. A new release of the International Terrestrial Reference Frame for earth science applications, *J. Geophys. Res.*, **107**, 2214, doi: 10.1029/2001JB000561.

Blewitt, G. & Lavallée, D., 2002. Effect of annual signals on geodetic velocity, *J. Geophys. Res.*, **107**, DOI 10.1029/2001JB000570.

Blewitt, G., Lavallee, D., Clarke, P., & Nurutdinov, K., 2001. A new global mode of earth deformation: Seasonal cycle detected, *Science*, **294**, 2342–2345.

Boucher, C., Altamani, Z., & Sillard, P., 1999. The International Terrestrial Reference Frame (ITRF97), IERS Technical Note 27, IERS, Observatoire de Paris, Paris.

Dong, D., Fang, P., Bock, Y., Cheng, M. K., & Miyazaki, S., 2002. Anatomy of apparent seasonal variations from GPS-derived site position time series, *J. Geophys. Res.*, **107**, xxx–xxx.

Kierulf, H. P., Kristiansen, O., & Plag, H.-P., 2001. Can GPS determine geocentric vertical crustal motion at the 1 mm/yr accuracy level?, in *Book of Extended Abstracts, Final Workshop of COST Action 40*, pp. 87–91, Hydrographic Institute of the Republic of Croatia - Split.

Kouba, J., 2003. A guide to using International GPS Service (IGS) products, IGS report, International GPS Service, available at ftp://igscb.jpl.nasa.gov/igscb/resource/pubs/GuidetoUsingIGSProducts.pdf.

McCarthy, D. D. & Petit, G., 2003. *IERS Conventions 2003*, IERS Technical Note 32, International Earth Rotation Service, In print. Available at http://www.iers.org.

Nikolaides, R. M., 2002. *Observation of geodetic and seismic deformation with the Global Positioning System*, Ph.D. thesis, University of California, San Diego.

Plag, H.-P., 2004. The IGGOS as the backbone for global observing and local monitoring: a user driven perspective, *J. Geodynamics*, In press.

Plag, H.-P. & Kierulf, H. P., 2005. Effect of unmodelled geocenter variations on global sea level trends, *Phys. Chem. Earth*, In press.

Ray, J., Dong, D., & Altamimi, Z., 2004. IGS reference frames: Status and future improvements, *GPS Solutions*, pp. DOI:10.1007/s10291–004–0110–x.

Scherneck, H.-G. & Bos, M. S., 2001. An automated internet service for ocean tidal loading calculations, http://www.oso.chalmers.se/ loading.

Wdowinski, S., Bock, Y., Zhang, J., & Fang, P., 1997. Southern California Permanent GPS geodetic array: spatial filterung of daily positions for estimating cosesimic and postseismic displacements induced by the 1992 Landers earthquake, *J. Geophys. Res.*, **102**, 18,057–18,070.

Wdowinski, S., Bock, Y., Baer, G., Prawirodirdjo, L., Bechor, N., Naaman, S., Knafo, R., Forrai, Y., & Melzer, Y., 2004. GPS measurements of current crustal movements along the Dead Sea Fault, *J. Geophys. Res.*, **109**, (B05403), 1–16.

Weber, R., 2001. IGS Electronic Mail 3605, Available at http://igscb.jpl.nasa.gov.

Zumberge, J. F., Heflin, M. B., Jefferson, D. C., & Watkins, M. M., 1997. Precise point positioning for the efficient and robust analysis of GPS data from large networks, *J. Geophys. Res.*, **102**, 5005–5017.